Journal of Power Sources 195 (2010) 4080–4089

Contents lists available at ScienceDirect

Journal of Power Sources

journal homepage: www.elsevier.com/locate/jpowsour

Dynamic response and long-term stability of a small direct methanol fuel cell stack

Young-Chul Park[a,c], Dong-Hyun Peck[a,*], Sang-Kyung Kim[a], Seongyop Lim[a], Doo-Hwan Jung[a], Jae-Hyuk Jang[b], Dok-Yol Lee[c]

[a] Korea Institute of Energy Research (KIER), 71-2 Jangdong, Yuseong, 305-343 Daejeon, Republic of Korea
[b] Electro Material and Device (eMD) Center, Samsung Electro-Mechanics Co., Maetan 3, Yeongtong, Suwon, 443-743 Gyeonggi, Republic of Korea
[c] Department of Advanced Materials Engineering, Korea University, 136-705 Seoul, Republic of Korea

ARTICLE INFO

Article history:
Received 15 October 2009
Received in revised form 1 December 2009
Accepted 1 January 2010
Available online 4 February 2010

Keywords:
Direct methanol fuel cell
Stack
Dynamic response
Interrupted operating method
Long-term test

ABSTRACT

This study examines the operating characteristics and durability of a small direct methanol fuel cell (DMFC) stack (volume: 39.6 cm^3). To investigate the operating characteristics in a real multi-user operating mode, various load cycles (such as gradual acceleration and deceleration), two operating modes (current mode or voltage mode) and four interrupted operating methods (load on–off, load–methanol on–off, load–air on–off, and load–methanol–air on–off) are used. The durability of the DMFC stack is examined at a constant voltage of 2.4 V (0.4 V per cell) by using the load–methanol–air on–off mode for more than 2000 h. In these tests, the DMFC stack exhibits a rapid, stable and dynamic response regardless of the load cycle and operating mode, though the stack performance and response behaviour vary with the interrupted operating modes. Among the operating modes, the air-interruption modes exhibit better stability and higher performance. Moreover, the load–methanol–air on–off mode provides the stack with good durability and a high performance in a long-term test of 2045 h.

1. Introduction

The direct methanol fuel cell (DMFC) is considered to be a promising power source for portable multi-functional electronic devices and light-duty vehicles because of its light weight, small size, high specific energy, and easy fuel storage capability [1–3]. The DMFC system, however, has several significant technical problems to be resolved, such as poor performance and methanol crossover. Accordingly, over the last decade, DMFC researchers have endeavoured to overcome the technical disadvantages through development of the proton-exchange membrane [4], the electrocatalyst [5,6], the bipolar plate [7], and the membrane electrode assembly (MEA) [8,9]. In spite of these numerous studies, several technical issues have still to be resolved for commercial applications, e.g., the durability of the fuel cell system [10] and the reliability and dynamic response in a real multi-user operating mode. These issues are of paramount importance in the design of a prototype system.

The long-term stability of MEAs is of significant concern due to degradation of cell components in either oxidizing or reducing environments that are induced by the cell reactions [11]. Many workers have examined the durability [10–17] and reliability (dynamic response) of the DMFC system [18–25]. Thomas et al. [26] studied several factors that affect the performance of DMFCs, focusing in particular on the long-term stability of the anode and the problem of methanol crossover. In that work, a life-span test at 0.4 V and 100 °C for 2000 h was conducted and showed a 12% loss in cell performance. It was suggested that the decay in the overall performance might be due to a slow drop in anode activity. Liu et al. [15] conducted a life-span test on a DMFC for 75 h at 100 mA cm^{-2} and found that 30% of the original maximum power density was lost. This performance degradation was attributed to agglomeration of the electrocatalysts and delamination of the MEA. Other researchers have also tried to determine the main parameters that govern the durability of DMFCs [27–37].

With regard to the dynamic response of DMFCs in a real multi-user operating mode, Argyropoulos et al. [18,19] emphasized not only transient operation that includes start-up and shut-down, but also the efficient transition between operating conditions for the development of engineering systems. They studied the dynamic response to consecutive changes and single-step changes in the current density and reported that the dynamic performance of the DMFC was affected by complex interactions between electrode kinetics and mass transport processes. Kallo et al. [24] observed the response of the cell voltage of a gas-feed DMFC to a step change in current density and reported the effect on the double-layer capacitance, the de-poisoning and poisoning of CO at the Pt catalyst of the anode, and the methanol crossover. Other researchers also investi-

* Corresponding author. Tel.: +82 42 860 3501; fax: +82 42 860 3739.
E-mail address: dhpeck@kier.re.kr (D.-H. Peck).

0378-7753/$ – see front matter © 2010 Elsevier B.V. All rights reserved.
doi:10.1016/j.jpowsour.2010.01.066

Table 1
Component specifications of DMFC stack.

MEA	
Membrane	Nafion 115
Catalyst of anode	PtRu/C, 1.8–2 Pt mg cm^{-2}
Catalyst of cathode	Pt/C, 1.5–1.6 Pt mg cm^{-2}
Thickness of MEA	510–530 μm
Active area of electrode	13.7 cm^2
MEA size	36 × 38 mm
Stack	
Number of cells	6 cell
Thickness of bipolar plate	1.5 mm
Size	48 × 50 × 16.5 mm
Thickness of gasket	200 μm
Total volume	39.6 cm^3

gated the dynamic behaviour of a DMFC by making a step change in the current density [20–23]. Recently, Yang and Zhao [38] developed a transient model to examine the dynamic response behaviour of a liquid-feed DMFC. The numerical results confirm that methanol permeation through the membrane produces a strong overshoot of the cathode overpotential, which is the predominant cause of voltage overshoot. By contrast, the anode overpotential is insensitive to changes in the methanol concentration and CO surface coverage in the anode catalyst layer.

Although there have been many advances in the durability and dynamic response of DMFCs, most of the reported studies have are focused on a single cell. Obviously, the results for a single cell can differ from those for a stack because each cell in the stack can exhibit different performance, fuel utility, mass transport, and methanol crossover. Thus, durability and dynamic response tests using a DMFC stack are necessary because practical systems use a stack. In addition, the operating characteristics must be examined to determine how a stack can be successfully managed in certain operating modes because this directly affects the durability of the DMFC system.

Accordingly, this investigation examines how the operating characteristics of a DMFC depend on various load cycles and operating modes; the durability with a small stack of 50.0 × 48.0 × 16.5 mm (volume: 39.6 cm^3) for a portable device is also studied.

2. Experimental

The MEA was fabricated with Nafion 115 as a proton-exchange membrane and with PtRu/C (Johnson Matthey) and Pt/C (Johnson Matthey) as electrocatalysts. For the gas-diffusion layers (GDLs) of the anode and cathode, Toray TGP060 and SGL 25BC carbon paper were used, respectively. The electrode layers were formed by applying a bar-coating method to the GDL with a catalyst slurry (comprised of Nafion ionomer and electrocatalysts). The Pt loading was 1.8–2 mg cm^{-2} for the anode and 1.5–1.6 mg cm^{-2} for the cathode.

The stack was fabricated with a small size of 50.0 × 48.0 × 16.5 mm (volume: 39.6 cm^3) for use in a digital multimedia broadcasting (DMB) phone with an output power of 5 W and a nominal voltage (2.4 V, 0.4 V per cell). The stack had six cells. Each cell had an active area of 13.7 cm^2 and internal manifolds for the supply of air and fuel. The bipolar plates, which had a thickness of 1.5 mm, were made from graphite by means of a computer numerical control lathe. A serpentine channel with two paths was used as the flow-field channel to supply air and a methanol solution to the stack. The component specifications of the DMFC stack are summarized in Table 1.

The operation characteristics of the DMFC stack were investigated with a test station (Wona Tech, Korea) equipped with an electronic load, a methanol pump, and an air pump. To evaluate the operating the characteristics of the stack in a real multi-user operating mode, various load cycles (such as gradual acceleration and deceleration), two operating modes (current or voltage mode), and four interrupted operating modes (load on–off, load–methanol on–off, load–air on–off, load–methanol–air on–off with an on-time of 30 min and an off-time of 10 s) were used.

Dynamic response tests of the stack voltage under an increasing current density step (from 0 to 200 mA cm^{-2}) are performed on two stack state (active state or inactive state). The stack is in an active state when the temperature is higher than 60 °C after consecutive operations.

In addition, to determine the optimum operating conditions for the DMFC stack, it was examined how a 1 M methanol solution (from λ = 1.5 (2.4 ml min^{-1}) to λ = 3.5 (5.3 ml min^{-1})) and air stoichiometry (λ = 1.5 (392 ml min^{-1}) to λ = 4 (1044 ml min^{-1})) affected the performance of the stack.

A durability test of the DMFC stack was performed at a constant voltage of 2.4 V (0.4 V per cell) with load–methanol–air on–off mode for more than 2000 h. After the long-term test, the changes in the stack performance were analyzed by the polarization curves, the voltage distribution of each cell, and the output power of each cell.

3. Results and discussion

The primary operating characteristics of the DMFC stack are show in Fig. 1. The DMFC stack shown in the photograph of Fig. 1(a) is designed in a U-shape, where the inlet and outlet are at the same side of the stack, so that it could be integrated with the balance-of-plant. Fig. 1(b) presents the polarization curves of the DMFC stack at different operating temperatures of 35 and 51 °C when a 1 M methanol solution (λ = 2.5) and air are supplied (λ = 3). At a low operating temperature of 35 °C, the stack has a maximum power output of 7.89 W (1.84 V at 4.29 A), a nominal power output of 6.31 W (2.4 V at 2.63 A), and a power density of 96 mW cm^{-2}. By contrast, when the stack operates at a high temperature of 51 °C, the stack performance significantly increases because the stack temperature enhances the kinetics of the electrochemical reaction [39]. At a high operating temperature of 51 °C, the stack has a maximum power output of 8.91 W (1.92 V at 4.64 A, 108 mW cm^{-2}), a nominal power output of 7.17 W (2.4 V at 2.99 A, 87 mW cm^{-2}), and a power density of more than 100 mW cm^{-2}. This stack exhibits much higher power output than the previous stack with the same electrode size and cell numbers [40], which had maximum power output of 7.63 W (1.81 V at 4.22 A, 93 mW cm^{-2}) and a nominal power output of 5.49 W (2.4 V at 2.29 A, 67 mW cm^{-2}). The results originate from improved MEA performance and component assembly method.

The voltage distribution of the six-cell stack at open-circuit voltage and a constant current of 2.8 A is given in Fig. 1(c). Each cell of the stack has a very uniform voltage distribution at 2.41 V and an open-circuit voltage of 4.99 V. This indicates that the fuel distribution inside the stack is homogeneous and the by-products of the reaction (H_2O and CO_2) are easily released. Such a uniform voltage distribution of cells in the stack would be advantageous in terms of the durability and the long-term stability of the stack. The starting opreation characteristics of the DMFC stack at a constant current of 2.82 A are presented in Fig. 1(d). The performance of the stack at the initial stage is affected by the temperature of the stack. As soon as the electric load is applied to the stack at room temperature, the voltage plunges by 2.05 V and then drastically escalates with increase in stack temperature. After 6 min, the voltage of the stack reaches 2.4 V and the output power remains between 6.74 and 6.85 W. This transient voltage possibly originates from the increased overpotential, which is attributed to an instant

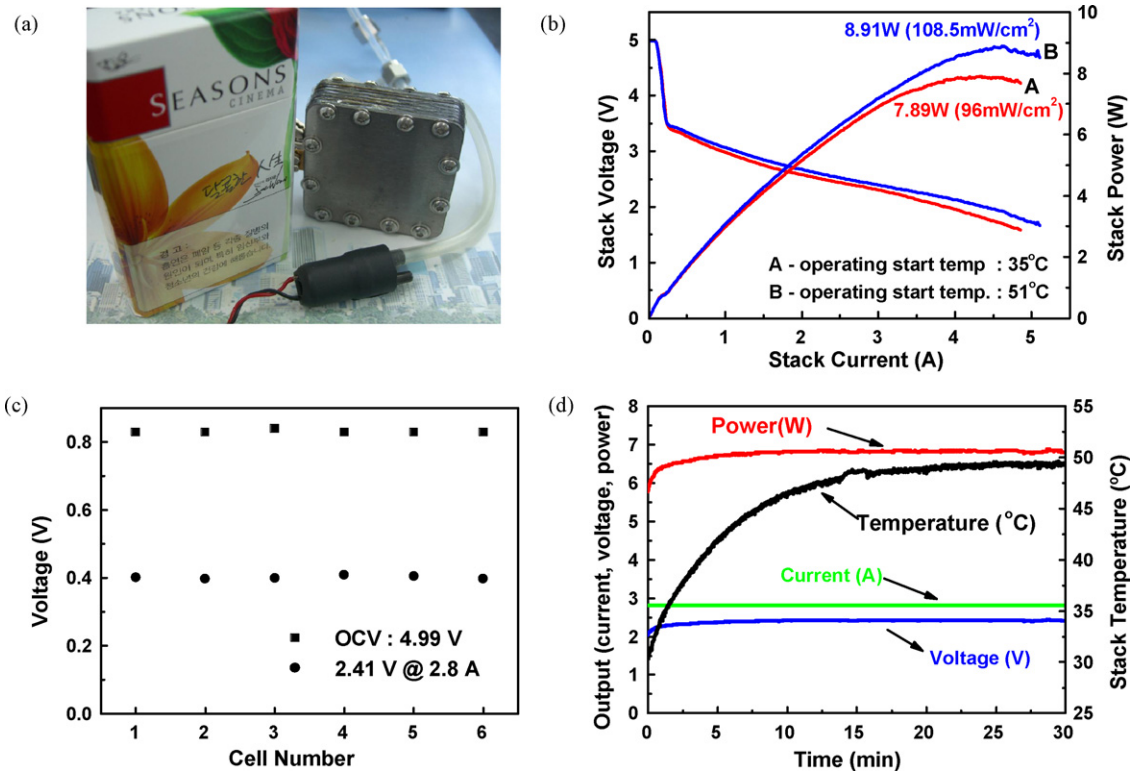

Fig. 1. Primary operating characteristics of DMFC stack: (a) photograph; (b) polarization curves; (c) voltage distribution at constant current of 2.8 A (fuel: 1 M CH_3OH, oxidant: air); (d) starting characteristics.

depletion of reactants in the electrodes and oxidization of absorbed poison species (such as CO_{ads} and CH_2OH_{ads}) on the catalyst surface [18–25]. Nevertheless, the DMFC stack has very stable operating characteristics; as soon as the stack begins to operate, it can provide an output power of 5.78 W. The high performance of the stack, the uniform voltage distribution and the stability imply that the stack components, including the MEA, the bipolar plates and the current-collector, are well designed and assembled. Detailed technical data of the DMFC stack are listed in Table 2.

The results of dynamic response tests of the fuel cell are given in Fig. 2. The dynamic response of the stack voltage under an increasing current density step (Fig. 2(a)) indicates the different transient responses that rely on the stack state (active state or inactive state) and the applied current density (from 0 to 200 mA cm^{-2}). When the stack is inactive, the voltage instantaneously drops below the steady-state and then gradually recovers from a meta-stable state. These phenomena are clear at a low current density below 75 mA cm^{-2}. According to previous studies, these phenomena are caused by a slow methanol oxidation reaction and a high overpotential that oxidizes adsorbed poisoning species such as CO_{ads} and CH_2OH_{ads} on the anode catalyst [18,19,24,25]. As the stack, however, shifts to a high current density, the voltage response is much faster because the temperature rises rapidly. This rise in temperature causes a fast methanol oxidation reaction and increases the vaporization of the aqueous phase, thereby enabling the methanol to penetrate the electrode layer easily as well as reducing the catalyst surface area that can be absorbed by the poisoning species.

When the stack is active after consecutive operations, the stack voltage response is much faster and more stable than that of an inactive stack for all current density ranges. Although a slight meta-stable state, such as overshooting and relaxation, occurs in a low current density range, the stack voltage instantly reaches a steady-state without a transient stage. These results indicate that the dynamic response of the stack is affected by the stack state and the applied current density that can govern the stack temperature, the methanol oxidation reaction (MOR), the catalyst utility, and two-path flow of reactants and products [18,19,24,25].

Fig. 3(a) and (b) shows the dynamic response of the DMFC stack as pulse currents of different magnitude are applied. In this

Table 2
Technical data of DMFC stack.

Operating temperature	35 °C	51 °C
Peak power	7.88 W	8.9 W
Nominal power (at 2.4 V)	6.33 W	7.17 W
Weight	106 g	106 g
Volume	39.6 cm^3	39.6 cm^3
Maximum current	4.86 A	5.11 A
Spec. peak power	199 W l^{-1} (74.3 W kg^{-1})	224.7 W l^{-1} (84 W kg^{-1})
Spec. nominal power	160 W l^{-1} (59.7 W kg^{-1})	181 W l^{-1} (67.4 W kg^{-1})

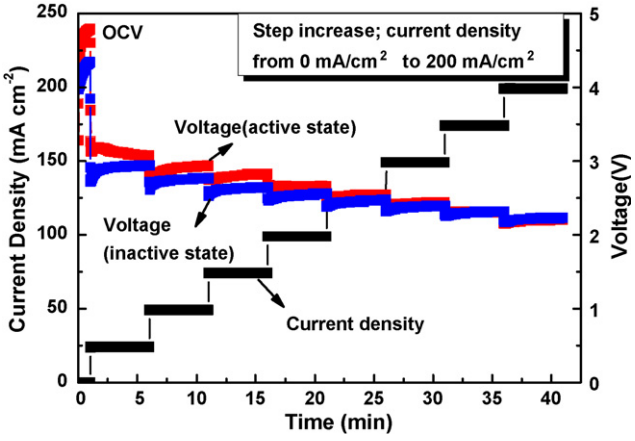

Fig. 2. Dynamic response of DMFC stack under increasing current density step (from 0 to 200 mA cm^{-2}).

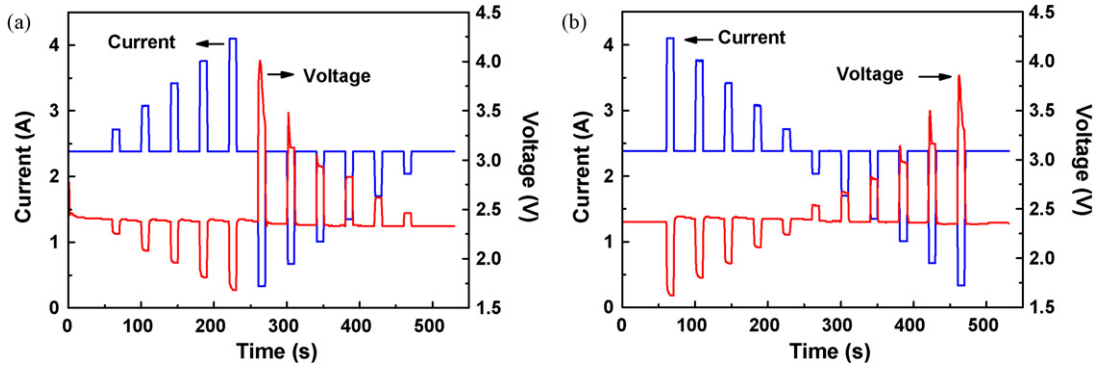

Fig. 3. Dynamic response of DMFC stack when pulse currents of different magnitude are abruptly applied to the stack and removed from the stack: (a) stack voltage response under gradually increasing pulse-current step; (b) stack voltage response under gradually decreasing pulse-current step.

experiment, when the stack is at a steady-state with a constant current of 2.4 A (around 2.4 V), various pulse-current steps from 0.33 A (24 mA cm^{-2}) to 4.1 A (300 mA cm^{-2}) are imposed on the stack for 10 s. As shown in Fig. 3(a) and (b), even though pulse currents of different magnitude are applied, the DMFC stack still has a rapid response rate regardless of the pulse current or the current intensity. The response behaviour of the DMFC stack, however, varies with the on–off state of the pulse current. If the pulse currents are removed, there is no problem because the DMFC stack instantly returns to a steady-state (around 2.4 V) and then exhibits very stable behaviour. When pulse currents, however, are imposed on the stack, the response behaviour depends on the applied pulse-current intensity. When pulse currents that are slightly higher (2.72–3.42 A, 200–250 mA cm^{-2}) or slightly lower (1.35–2.04 A, 100–150 mA cm^{-2}) than the operating current of 2.4 A (175 mA cm^{-2}) are applied, the stack instantly reaches a steady-state without a transient stage. If, however, pulse currents that are much higher (3.76–4.1 A, 275–300 mA cm^{-2}) or much lower (0.34–1.01 A, 25–75 mA cm^{-2}) than the operating current are applied, relaxation or overshooting in the dynamic responses is observed and the stack voltage reaches a steady-state after a transient stage of 2–8 s. Especially when a very low pulse current (0.34–1.01 A, 25–75 mA cm^{-2}) is applied, the stack experiences very high overshooting and a relatively slow response to a steady voltage. According to Kallo et al. [24], the stack voltage increase occurs because the excess catalyst surface, which delivers the low current density, is poisoned when the lower current density has to be generated from complete methanol dehydrogenation and CO_{ads} oxidation. The longer relaxation times with decreasing current density are based on the non-linear behaviour of the charge-transfer resistance, which causes the relaxation time for the double-layer capacitance to depend on the end value of the current density. In summary, the above findings confirm that if the DMFC stack operates at a constant current of 2.4 A (around 2.4 V), the stable operating current is in the range of 1.35 A (100 mA cm^{-2}) to 3.42 A (250 mA cm^{-2}). This performance is adequate for the good stack stability and fast dynamic response.

Besides the dynamic response, it is necessary to address the stack operating mode as this may significantly influence the stack performance and stability. If consecutive operations of the DMFC stack are limited to a few 10 min periods, the performance is less likely to deteriorate because of reduction of catalyst poisoning, catalyst fatigue, water flooding, and so on. According to Neergat et al. [41], a pulse method can improve the performance of a DMFC in low current density. They suggested that after the pulse, the anode potential is shifted positive to the onset potential for CO_{ads} oxidation and that the H_{ads} oxidation can proceed at a larger number of free surface sites. Nevertheless, the performance of a DMFC cannot be maintained solely with the pulse method for a long time due to the mass transport problem, water flooding, and Pt catalyst oxidation. Eickes et al. [42] used an 'air break' method to investigate the performance of the DMFC cathode. This method lowers the cathode potential below the value required for complete reduction of the electrode surface. Accordingly, the experimental results confirm that an appropriate interrupted operating mode can be used to operate a stack safely for a few thousand hours.

Fig. 4 shows the dynamic response of the DMFC stack to the different interrupted operating modes at a constant current of 2.4 A. These operating modes have the same load-on time (120 s) and load-off time (10 s), whereas the fuel supply condition during the load-off time varies with the given operating mode. The data in Fig. 4(a) show that the stack performance and response behaviour are affected by the interrupted operating modes. When the DMFC stack is operated by a load on–off mode and a load-methanol on–off mode, the stack has an output power of 5.11 W. By contrast, the stack performance is greatly increased above 6 W when the DMFC stack is operated by a load–air on–off mode and a load–methanol–air on–off mode. These results demonstrate that the difference in performance of the DMFC stack for the various operating modes is caused by air interruption at the cathode. The increase of the performance is probably related to efficient removal of water in the cathode by the air on–off process. This, however, fails to explain why a short cycling time produces a performance difference of 1 W. It is therefore assumed that complex electrochemical reactions on catalysts, such as catalyst poisoning and de-poisoning and a catalyst utility, are affected by rapid voltage changes under the interrupted operating modes. The hypothesis can be supported by the subsequent dynamic response behaviour with these operating modes.

As shown in Fig. 4(b) and (c), the generated stack current varies with the operating modes. In addition, the operating modes display different current (Fig. 4(b)) and voltage response behaviour (Fig. 4(c)). With regard to the stack current response, when the stack is operated by the load on–off mode and the load–methanol on–off mode, the current reaches a steady-state without a transient stage. By contrast, when operated by the load–air on–off mode and the load–methanol–air on–off mode, the stack undergoes an overshooting and relaxation process. Note that the load–methanol–air on–off mode gradually increases the current in the initial regime and then the stack returns to a steady-state. These transients are similar to the results of Neergat et al. [41] for a low current density of 60 mA cm^{-2}. They demonstrated that the rise in current can be reasonably explained by the de-poisoning of the electrode surface through oxidation of CO-like adsorbents; the de-poisoning produces more free surface sites for the parallel path of the methanol oxidation reaction. Hence, the load–air on–off mode and the load–methanol–air on–off mode appear to be effective

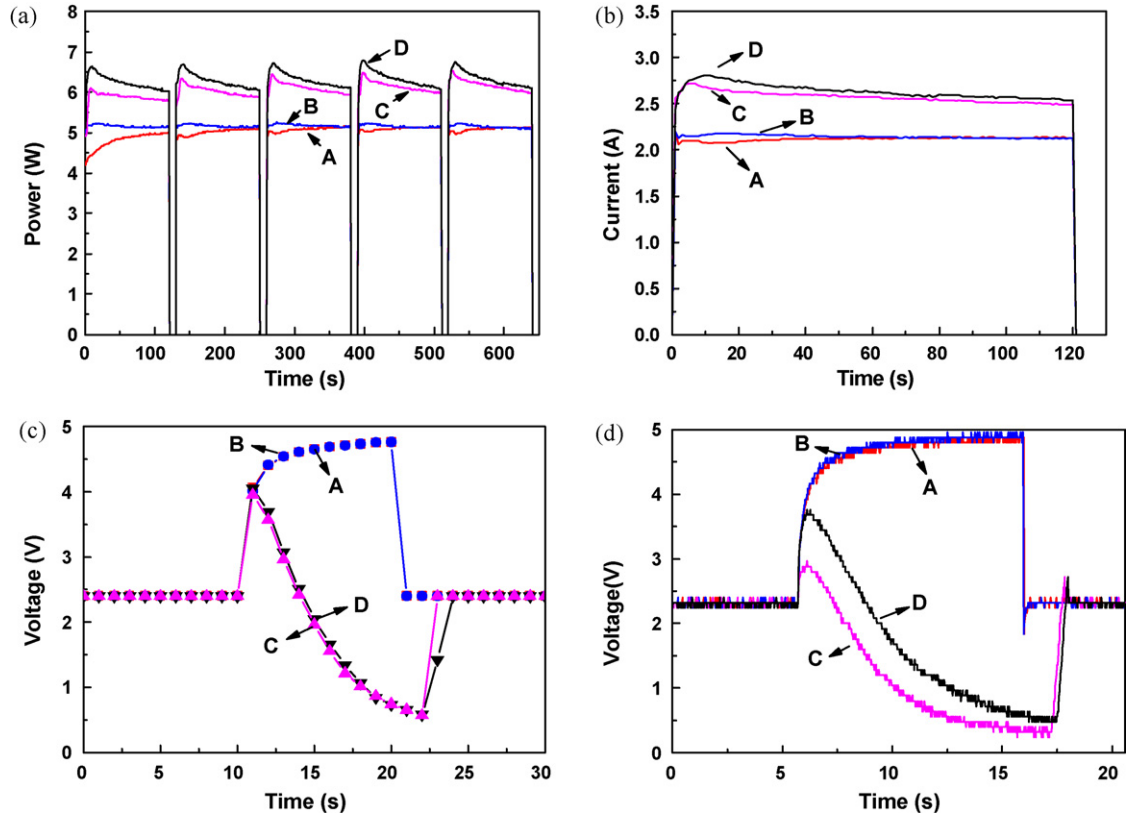

Fig. 4. Dynamic response of DMFC stack in relation to operating mode: (a) stack performance; (b) current response for on–off state; (c) voltage response for on–off state (sampling time: 1 s); (d) voltage response for on–off state measured with oscilloscope (sampling time: 0.02 s); A: load on–off mode; B: load–methanol on–off mode; C: load–air on–off mode; D: load–methanol–air on–off mode.

in increasing the active sites of the catalyst. These phenomena originate from the stack voltage behaviour during the load-off state.

When the stack is in the off-state of the load on–off mode and the load–methanol on–off mode, the voltage returns to the open-circuit value. By contrast, the voltage falls to around 0.5 V in the off-state of the load–air on–off mode and the load–methanol–air on–off mode (as shown in Fig. 4(c)). According to previous reports [43,44], at high positive potentials, a Pt oxide layer forms due to the oxidation of Pt itself or corrosion of the carbon support occurs and it decreases the number of Pt active sites. On the other hand, a low potential at the cathode (below 0.5 V versus RHE) can fully reduce the surface oxide of the Pt catalyst and rapidly consume oxygen at the cathode, and thereby lead to possible recovery of the performance of the DMFC cathode [42]. Therefore, the voltage drop under the load-off state appears to promote de-poisoning of the catalyst surface, and it promotes better performance of the stack under the load–air on–off mode and the load–methanol–air on–off mode.

It should be also noted that when the load–air on–off mode and the load–methanol–air on–off mode are applied, the stack retains a low voltage for 2–3 s in the load-on state. In addition, when the air-interruption modes are used, the air supply in the cathode is delayed for 2–3 s. Thus, instantaneous air-starving in the cathode can lower the cathode potential required for subsequent reduction of the surface oxide [42]. Furthermore, even if the air supply flowing into the stack is delayed, the stack produces a high current. This phenomenon can occur because the residual air in stack channels or the porous layers of the electrode participates in the reaction (which requires 8.7–13 cm^3 of air at 2.5 A), and also because the double-layer capacitance at both electrodes discharges a higher current.

The voltage responses of the DMFC stack in an on–off state as measured with an oscilloscope are shown in Fig. 4(d). The measurements were taken in a very short sampling time of 0.02 s so that more detailed voltage behaviour could be observed. Unlike the voltage responses of the on–off state measured by the test station (with a sampling time of 1 s), transient and overshooting behaviour (around 16 and 18 s) can be observed at the voltage responses even if the stack is operated at a constant voltage of 2.4 V. As indicated in Figs. 2 and 3, the transient stage is due to a high overpotential to oxidize the adsorbed poison species, and the overshooting arises from the poisoning of the excess catalyst sur-

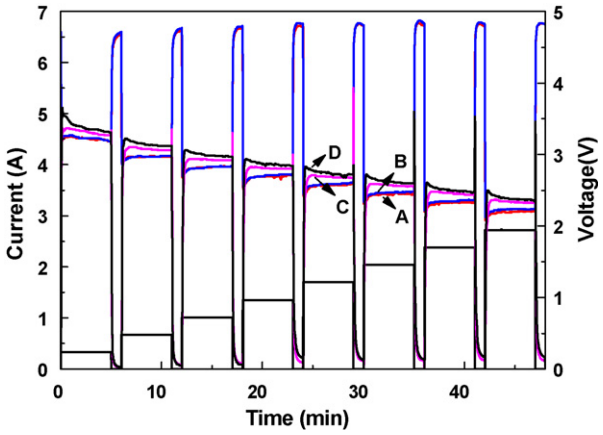

Fig. 5. Dynamic response of DMFC stack in relation to different interrupted operating modes under stepwise increasing pulse-current condition; A: load on–off mode; B: load–methanol on–off mode; C: load–air on–off mode; D: load–methanol–air on–off mode.

face. These results imply that, during the off-state, the load on–off mode and the load–methanol on–off mode induce catalyst poisoning, whereas the load–air on–off mode and the load–methanol–air on–off mode induce catalyst de-poisoning. Therefore, all the data in Fig. 4 support the view that the load–air on–off mode and the load–methanol–air on–off mode are superior operating modes for the DMFC stack than the load on–off mode and the load–methanol on–off mode.

The dynamic response of a DMFC stack in relation to different interrupted operating modes under a stepwise increasing pulse-current condition is presented in Fig. 5. When the pulse currents are imposed, the DMFC stack shows the same dynamic responses at an operating mode regardless of the pulse-current intensity. The dynamic response behaviour of the stack, however, varies significantly with the operating mode. For the load on–off mode and the load–methanol on–off mode, the voltage instantaneously plummets and then returns to a steady-state. For the load–air on–off mode, however, the voltage gradually increases for 30 s to reach a steady-state. Finally, the load–methanol–air on–off mode induces overshooting, and requires a longer time to return to a steady-state. Similar behaviour is observed at every pulse current. These findings demonstrate that the operating modes of the DMFC also influence the dynamic responses of the stepwise increasing pulse currents. As mentioned above, this influence may be caused by catalyst poisoning and de-poisoning during the load-off state. Yang et al. [38] examined the dynamic response behaviour when the load changes from a high to a low current density. They reported that as the current density plummets, the number of free Pt catalyst sites exceeds the number required for complete methanol oxidation; hence, methanol adsorption and the dehydrogenation step prevail over conversion of CO to CO_2, and consequently cause an increase in the surface coverage of CO on the Pt catalyst at the anode. On

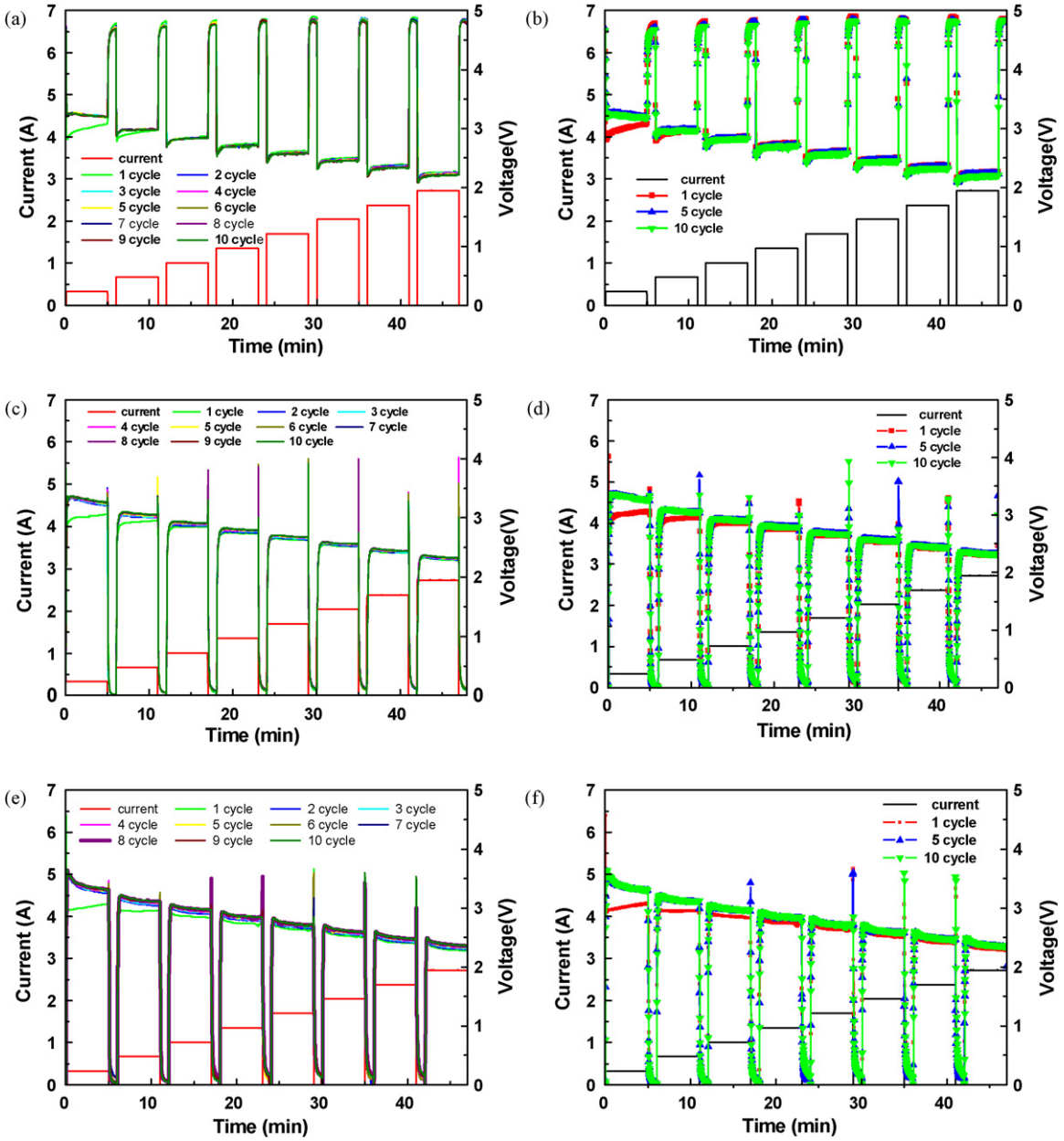

Fig. 6. Cyclic dynamic tests of DMFC stack in relation to different interrupted operating modes under increasing pulse-current condition: (a) and (b) load–methanol on–off mode; (c) and (d) load–air on–off mode; (e) and (f) load–methanol–air on–off mode. (Cycle dynamic response of load on–off mode is equivalent to results of load–methanol on–off mode.)

the basis of their results, it is assumed that the load and fuel on–off mode has more free Pt catalyst sites than the other modes and that free Pt catalyst sites are formed during the load-off state.

The cyclic dynamic response of a DMFC stack under a stepwise increasing pulse-current condition is reported in Fig. 6. The response is tested over 10 cycles in order to evaluate the stability of the stack under the interrupted operating modes (Fig. 6(a), (c) and (e)). During these tests, the stack exhibits a uniform response for all operating modes and all pulse currents. The stack is very stable and responds rapidly under various pulse currents, regardless of the operating mode. These cyclic dynamic responses are in good agreement with the results of Fig. 5. As the number of cyclic dynamic tests increase from 1 to 10 cycles (Fig. 6(b), (d) and (f)), the voltage of the stack operated by the load on–off mode and the load–methanol on–off mode tends to decrease slightly (Fig. 6(b)), whereas the voltage of the stack operated by the air-interruption modes remains constant (Fig. 6(d)) or increases slightly (Fig. 6(f)). These phenomena can be explained by the above-mentioned reasons, such as catalyst poisoning, catalyst de-poisoning, and the number of free Pt catalyst sites. In addition, the 8 h cycle test suggests that the phenomena could originate from differences in the capability to remove the water produced or accumulated at the cathode. This capability can limit the mass transport and reduce the catalyst utilization. In other words, during the cyclic test, the air-interruption modes can continually discharge the water in the cathode by means of the air on–off process. Such water removal plays an important role in preserving the performance of the fuel cell. It indicates that the air-interruption mode is more stable as a DMFC operating method than the other modes.

The results of a 100 h stability test of the DMFC stack with the load on–off mode and the load–methanol–air on–off mode are given in Fig. 7. The test is performed at a constant voltage of 2.4 V (0.4 V per cell) to compare the stability and durability of the two operating modes. For both these modes, the load-on time is 30 min and the load-off time is 10 s. A 1 M methanol solution and air are supplied with $\lambda = 2.2$ and $\lambda = 2.5$, respectively. According to the results, when the DMFC stack is operated in the load–methanol–air on–off mode, the performance (average output power: 7.07 W, 86 mW cm^{-2}) is constant for 100 h. On the other hand, when the stack is operated in the load on–off mode, the performance (average output power: 6.4 W, 78 mW cm^{-2}) diminishes slightly at a rate of $y = -0.0436x + 6.617$ (y = power (W), x = time (h)). These observations, which are consistent with the results of the cyclic dynamic response test, prove that the load–methanol–air on–off mode is better as a long-term operating method than a general load on–off mode.

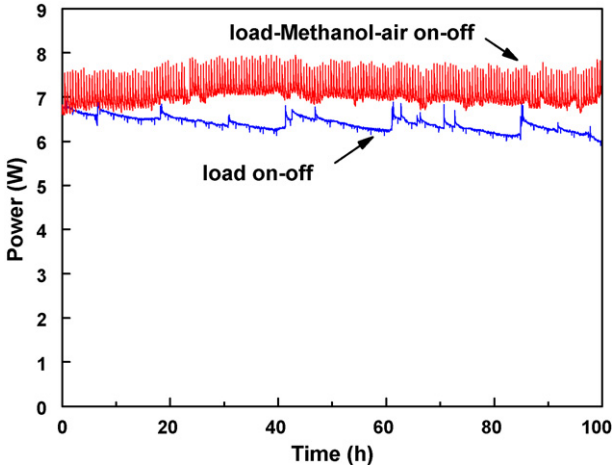

Fig. 7. Stability test of DMFC stack with load–methanol–air on–off mode and load on–off mode.

During the 10 s cessation of the load, in load–methanol–air on–off operation, methanol and air produce repetitive peaks on the power versus time plot. As indicated in Figs. 5 and 6, this behaviour is due to the high overshooting and slow relaxation process of the load–methanol–air on–off operation. Even though the operating mode continually induces an unsteady state of the DMFC stack, it can improve the reliability and durability of the stack, and ensure high performance. Hence, the load–methanol–air on–off operation can operate a DMFC more stably over a long period than the other operating modes.

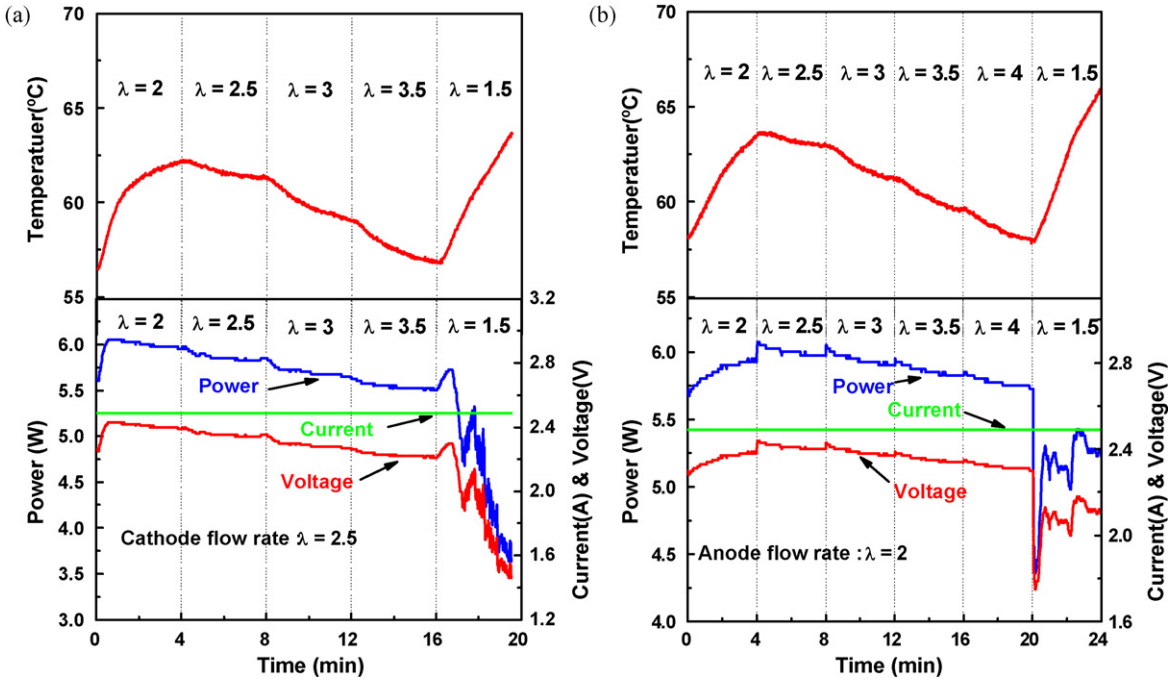

Fig. 8. Effects of fuel stoichiometry on stack performance: (a) methanol stoichiometry; (b) air stoichiometry.

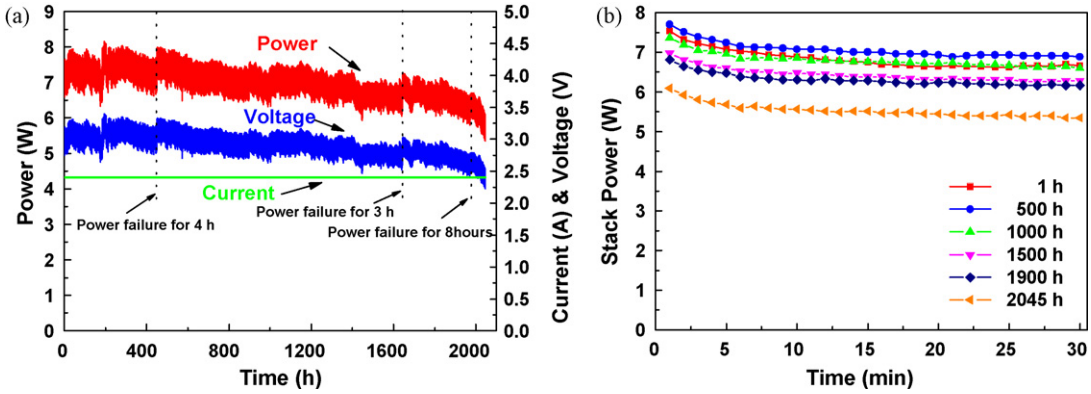

Fig. 9. (a) Long-term test of DMFC stack with load–methanol–air on–off mode at constant voltage of 2.4 V for 2045 h; (b) power variation under load-on state during long-term test.

The effects of fuel stoichiometry on stack performance at a constant current of 2.5 A are given in Fig. 8. During DMFC stack operation, the amount of fuel fed into the stack is as important as the operating mode because it can determine the fuel distribution, the fuel efficiency and methanol crossover, the stack temperature change, and DMFC operating characteristics such as performance and durability. When air is supplied at a flow rate of $\lambda = 2.5$ (653 ml min^{-1}) and the flow rate of the 1 M methanol solution is changed from $\lambda = 1.5$ (2.4 ml min^{-1}) to $\lambda = 3.5$ (5.3 ml min^{-1}), the stack performance diminishes as the flow rate of the supplied methanol increases, see Fig. 8(a). This result is due to a decline in stack temperature as well as higher methanol crossover. Between $\lambda = 2$ and $\lambda = 3.5$, the stack temperature drops by about 5 °C, thereby inducing a poorer stack performance. The stack exhibits the highest performance and stability at $\lambda = 2$ (3.1 ml min^{-1}). This suggests that although a small quantity of methanol is supplied into a stack, the fuel distribution is very uniform in each cell. Such uniformity is very beneficial to the long-term operation of the stack, and the reduced methanol crossover improves the fuel efficiency. Nevertheless, when the methanol flow rate is at $\lambda = 1.5$, the voltage falls and the stack performance decreases significantly because the resultant lack of methanol solution causes an imbalance in the fuel distribution. These findings therefore indicate that a methanol flow rate of $\lambda = 2$ (3.1 ml min^{-1}) is the optimum operating condition in terms of fuel efficiency and the long-term operation of the stack. Similarly, when a 1 M methanol solution is supplied at a flow rate of $\lambda = 2$ (3.1 ml min^{-1}) and the flow rate of air is changed from $\lambda = 1.5$ (392 ml min^{-1}) to $\lambda = 4$ (1044 ml min^{-1}) (Fig. 8(b)), the transient performance of the stack is affected by a change in the air flow rate. The stack performance linearly decreases when the air flow rate increases because of a fall in the stack temperature. At $\lambda = 2.5$, the stack exhibits its highest performance and stability. On the other hand, when air is supplied at a flow rate of $\lambda = 1.5$, the voltage decreases abruptly due to the lack of air supply inside the stack. This

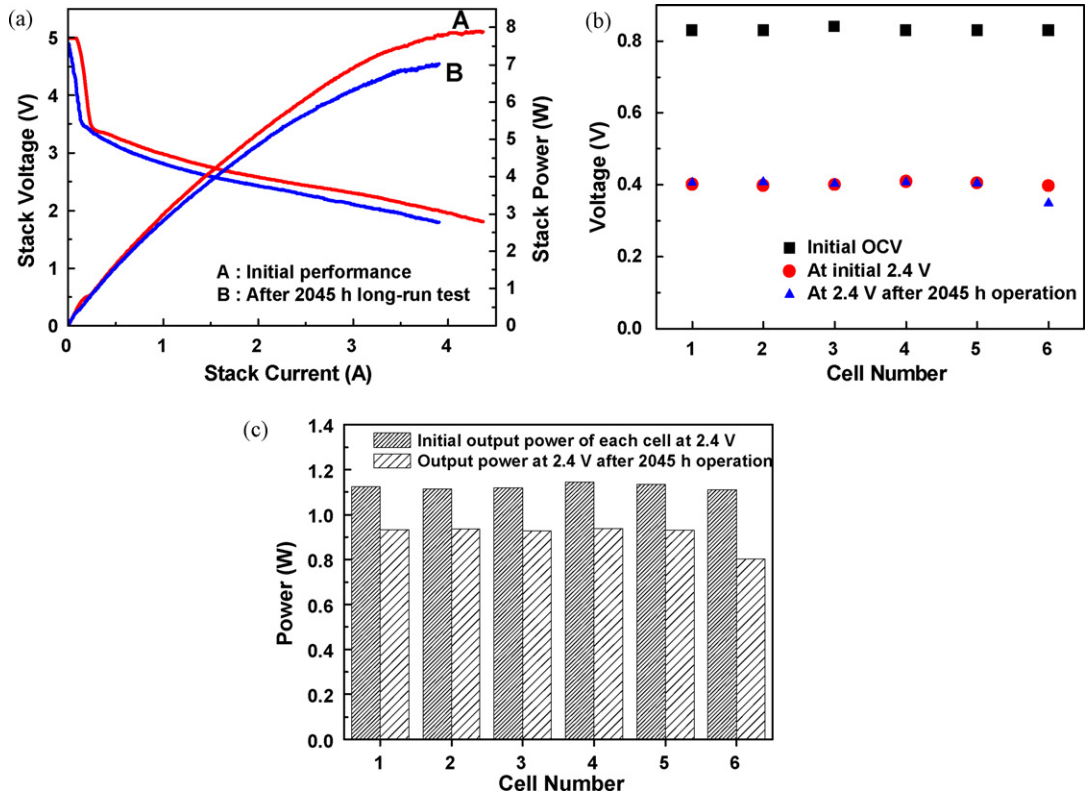

Fig. 10. Polarization curve of stack (a), voltage distribution (b), output power of each cell (c) after long-term test of 2045 h.

behaviour means that the air in each cell of the stack is insufficient and non-uniform. Thus, an air flow rate of $\lambda = 2.5$ (653 ml min^{-1}) is required for safe operation of the DMFC stack.

Given that the operating characteristics of the DMFC depend on the operating mode and fuel stoichiometry, a long-term test (2045 h) on a DMFC stack has been performed by using the load–methanol–air on–off operation with a methanol flow rate of $\lambda = 2$ (3.1 ml min^{-1}) and an air flow of $\lambda = 2.5$ (653 ml min^{-1}).

The results are presented in Fig. 9(a) and the power variation in the load-on state (30 min) are reported in Fig. 9(b). The test was performed at a constant voltage of 2.4 V. The external electricity failed three times during the long-term operation, as indicated in Fig. 9. The results show that even though the DMFC stack is operated in high current densities between 170 and 245 mA cm^{-2}, it maintains a high performance above 5.5 W for more than 2000 h by using the load–methanol–air on–off operation. As demonstrated in Fig. 7, although the operating mode continually induces an unsteady state in the stack due to repetitive overshooting and relaxation (Fig. 9(b)), it enhances the performance stability of the stack throughout the long-term test. This indicates that the load–methanol–air on–off operation is a good operating procedure for prolonging the life of a DMFC. At the beginning of the test, the stack provides 6.83 W (83 mW cm^{-2}) of power and this output is maintained for 1350 h; the power then drops to 5.54 W (67 mW cm^{-2}). The observed performance loss over the 2045 h period is about 19%. It should be noted, however, that most of the performance decline occurs after 1900 h, whereas the performance loss is 7.8% (6.3 W, 77 mW cm^{-2}) before 1900 h (Fig. 9(b)). The latter performance decline is possibly caused by a reduction in the active surface area and poisoning of the MEA components.

The polarization curve of the stack is given in Fig. 10(a), the voltage distribution in Fig. 10(b), and the output power of each cell in Fig. 10(c) after the long-term test of 2045 h. The polarization curve in the stack shifts in a vertical direction due to a reduction of the active surface area. As a result, the performance of the stack declines from the initial level of 7.9 to 7.02 W (1.8 V at 3.9 A). The performance loss for a nominal voltage of 2.4 V is about 20%, which is similar to the value obtained in Fig. 9. When compared with the maximum power output, the performance loss decreases by about 11.2%.

With regard to the voltage distribution of the six-cell stack at 2.4 V (Fig. 10(b)), the sixth cell, which is the farthest cell from the fuel inlet and outlet, has a much lower voltage whereas the other cells show very uniform voltage. This phenomenon may be due to the fuel flow through the stack. The stack is designed in a U-shape. Therefore, the last cell has a long pathway for the supply of fuels and the removal of by-products (H_2O and CO_2). Hence, as the operating time of the stack progresses, the last cell experiences difficulties with regard to the supply of fuel and the release of the produced H_2O and CO_2. Such problems of the last cell explain the degradation in stack durability and performance during long-term operation. Consequently, the output power of each cell after the long-term test of 2045 h is the same as the results of the voltage distribution. As shown in Fig. 10(c), the performance of the sixth cell (about 10 mW cm^{-2}) is much lower than that of the other cells.

4. Conclusions

The dynamic response of a DMFC stack is affected by the stack state and the applied current density that govern complex interactions such as the stack temperature, the methanol oxidation reaction (MOR), and the catalyst utility. Even though pulse currents of different magnitude are instantaneously applied to the stack, the DMFC shows a very fast response rate, regardless of the pulse current and the current intensity. When the stack is operated at a constant current of 2.4 A (around 2.4 V), the stable operating current range of the stack varies from 1.35 A (100 mA cm^{-2}) to 3.42 A (250 mA cm^{-2}).

The stack performance and response behaviour, however, vary with the interrupted operating mode. This is because the operating mode significantly influences the complex electrochemical reactions, particularly the poisoning or de-poisoning of species (CO_{ads} and CH_2OH_{ads}) absorbed on the catalyst surface. The air-interruption modes (the load–air on–off mode and the load–methanol–air on–off mode) provide better stability and performance than the other modes. Specifically, for both these air-interruption modes, the H_{ads} oxidation proceeds at a larger number of free surface sites and the performance of the DMFC cathode is recovered since the lower potential of the cathode induces complete reduction of the electrode surface.

Under long-term operation with the load–methanol–air on–off mode, the observed performance loss over 2045 h is about 19% (6.83 W → 5.54 W). Most of the performance decline occurs after 1900 h, i.e., the performance loss is 7.8% (6.3 W, 77 mW cm^{-2}) before 1900 h. This decline is attributed to the performance degradation of the sixth cell which is the farthest cell from the fuel inlet and outlet.

Acknowledgements

This work was supported by the Renewable Energy RD&D Programs for Fuel Cells of the Ministry of Knowledge Economy (MKE) of Korea.

References

[1] X. Ren, P. Zelenay, S. Thomas, J. Davey, S. Gottesfeld, J. Power Sources 86 (2000) 111–116.
[2] M. Broussely, G. Archdale, J. Power Sources 136 (2004) 386–394.
[3] H. Dohle, H. Schmitz, T. Bewer, J. Mergel, D. Stolten, J. Power Sources 106 (2002) 313–322.
[4] A. Ainla, D. Brandell, Solid State Ionics 178 (2007) 581–585.
[5] K. Nam, D.H. Jung, S.K. Kim, D.H. Peck, S.K. Ryu, J. Power Sources 173 (2007) 149–155.
[6] H. Yamada, T. Hirai, I. Moriguchi, T. Kudo, J. Power Sources 164 (2007) 538–543.
[7] S. Arisetty, A.K. Prasad, S.G. Advani, J. Power Sources 165 (2007) 49–57.
[8] J. Zhang, G. Yin, Z. Wang, Y. Shao, J. Power Sources 160 (2006) 1035–1040.
[9] H. Tang, S. Wang, M. Pan, S.P. Jiang, Y.Z. Ruan, Electrochim. Acta 52 (2007) 3714–3718.
[10] J.Y. Park, J.H. Lee, J.H. Sauk, I.H. Son, Int. J. Hydrogen Energy 33 (2008) 4833–4843.
[11] L.S. Sarma, C.H. Chena, G.R. Wang, K.L. Hsueh, C.P. Huang, H.S. Sheu, D.G. Liu, J.F. Lee, B.J. Hwang, J. Power Sources 167 (2007) 358–365.
[12] A.K. Shukla, C.L. Jackson, K. Scott, R.K. Raman, Electrochim. Acta 47 (2002) 3401.
[13] J. Liu, Z. Zhou, X. Zhao, Q. Xin, G. Sun, B. Yi, Phys. Chem. Chem. Phys. 6 (2004) 134.
[14] S.D. Knights, K.M. Colbow, St. Pierre, D.P. Wilkinson, J. Power Sources 127 (2004) 127–134.
[15] J. Liu, Z. Zhou, X. Zhao, Q. Xin, G. Sun, B. Yi, Phys. Chem. Chem. Phys. 6 (2004) 134–137.
[16] W. Chen, G. Sun, J. Guo, X. Zhao, S. Yan, J. Tian, Electrochim. Acta 51 (2006) 2391–2399.
[17] M.K. Jeon, K.R. Lee, K.S. Oh, D.S. Hong, J.Y. Won, S. Li, J. Power Sources 158 (2006) 1344–1347.
[18] P. Argyropoulos, K. Scott, J. Power Sources 87 (2000) 153.
[19] P. Argyropoulos, K. Scott, Electrochim. Acta 45 (2000) 1983.
[20] A. Simoglou, P. Argyropoulos, Chem. Eng. Sci. 56 (2001) 6761.
[21] A. Simoglou, P. Argyropoulos, Chem. Eng. Sci. 56 (2001) 6773.
[22] A.A. Kulikovsky, Electrochem. Commun. 3 (2001) 572.
[23] K. Sundmacher, T. Schultz, Chem. Eng. Sci. 56 (2001) 333.
[24] J. Kallo, J. Kamara, W. Lehnert, R. Helmolt, J. Power Sources 127 (2004) 181–186.
[25] J.H. Yoo, H.G. Choi, J.D. Nam, Y.K. Lee, C.H. Chung, E.S. Lee, J.K. Lee, S.M. Cho, J. Power Sources 158 (2006) 13–17.
[26] S.C. Thomas, X. Ren, S. Gottesfeld, P. Zelenay, Electrochim. Acta 47 (2002) 3741.
[27] J.T. Mueller, P.M. Urban, J. Power Sources 75 (1998) 139–143.
[28] C.S. Kong, D.Y. Kim, H.K. Lee, Y.G. Shul, T.H. Lee, J. Power Sources 108 (2002) 185–191.
[29] D.A. Blom, J.R. Dunlap, T.A. Nolan, L.F. Allard, J. Electrochem. Soc. 150 (2003) A414–A418.
[30] T. Romero-Castanon, L.G. Arriaga, Y. Cano-Castillo, J. Power Sources 118 (2003) 179–182.

[31] H.S. Chu, C.Y. Yeh, F. Chen, J. Power Sources 123 (2003) 1–9.
[32] J.S. Lee, K.I. Han, S.O. Park, H.N. Kim, H. Kim, Electrochim. Acta 50 (2004) 807–810.
[33] M. Schulze, A. Schneider, E. Gulzow, J. Power Sources 127 (2004) 213–221.
[34] M. Parasana, H.Y. Ha, E.A. Cho, S.A. Hong, I.H. Oh, J. Power Sources 131 (2004) 147–154.
[35] C. Lim, C.Y. Wang, Electrochim. Acta 49 (2004) 4149–4156.
[36] P. Piela, C. Eickes, E. Brosha, F. Garzon, P. Zelenay, J. Electrochem. Soc. 151 (2004) A2053–A2059.
[37] H. Kim, S.J. Shin, Y.G. Park, J.H. Song, H.T. Kim, J. Power Sources 160 (2006) 440–445.
[38] W.W. Yang, T.S. Zhao, J. Power Sources 185 (2008) 1131–1140.
[39] J. Ge, H. Liu, J. Power Sources 142 (2005) 56–69.
[40] Y.C. Park, D.H. Peck, D.H. Jung, S.K. Kim, S.Y. Lim, B.D. Lee, J.H. Jang, D.R. Lee, ECS Trans. 16 (2008) 801–805.
[41] M. Neergat, T. Seiler, E.R. Savinova, U. Stimming, J. Electrochem. Soc. 153 (2006) A997–A1003.
[42] C. Eickes, P. Piela, J. Davey, P. Zelenay, J. Electrochem. Soc. 153 (2006) A171–A178.
[43] U.A. Paulus, T.J. Schmidt, H.A. Gasteiger, R.J. Behm, J. Electroanal. Chem. 495 (2001) 134–145.
[44] Y. Shao, G. Yin, Y. Gao, P. Shi, J. Electrochem. Soc. 153 (2006) A1093–A1097.